University of Huddersfield Repository

Zhang, Tao, Gao, Feng and Jiang, Xiangqian

A surface topography acquisition method for double-sided near-right-angle structured surfaces based on dual-probe wavelength scanning interferometry

Original Citation

Zhang, Tao, Gao, Feng and Jiang, Xiangqian (2017) A surface topography acquisition method for double-sided near-right-angle structured surfaces based on dual-probe wavelength scanning interferometry. Optics Express, 25 (20). pp. 24148-214156. ISSN 1094-4087

This version is available at http://eprints.hud.ac.uk/id/eprint/33425/

http://eprints.hud.ac.uk/

Check for updates

Surface topography acquisition method for double-sided near-right-angle structured surfaces based on dual-probe wavelength scanning interferometry

TAO ZHANG, FENG GAO,[*] AND XIANGQIAN JIANG

University of Huddersfield, Huddersfield, UK
* F.Gao@hud.ac.uk

Abstract: This paper proposes an approach to measure double-sided near-right-angle structured surfaces based on dual-probe wavelength scanning interferometry (DPWSI). The principle and mathematical model is discussed and the measurement system is calibrated with a combination of standard step-height samples for both probes vertical calibrations and a specially designed calibration artefact for building up the space coordinate relationship of the dual-probe measurement system. The topography of the specially designed artefact is acquired by combining the measurement results with white light scanning interferometer (WLSI) and scanning electron microscope (SEM) for reference. The relative location of the two probes is then determined with 3D registration algorithm. Experimental validation of the approach is provided and the results show that the method is able to measure double-sided near-right-angle structured surfaces with nanometer vertical resolution and micrometer lateral resolution.

References and links

1. X. Zhang, L. Jiang, Z. Zeng, F. Fang, and X. Liu, "High angular accuracy manufacture method of micro v-grooves based on tool alignment by on-machine measurement," Opt. Express **23**(21), 27819–27828 (2015).
2. D. Li, C. F. Cheung, M. Ren, L. Zhou, and X. Zhao, "Autostereoscopy-based three-dimensional on-machine measuring system for micro-structured surfaces," Opt. Express **22**(21), 25635–25650 (2014).
3. D. Li, C. F. Cheung, M. Ren, D. Whitehouse, and X. Zhao, "Disparity pattern-based autostereoscopic 3D metrology system for in situ measurement of microstructured surfaces," Opt. Lett. **40**(22), 5271–5274 (2015).
4. D. Purcell, A. Suratkar, A. Davies, F. Farahi, H. Ottevaere, and H. Thienpont, "Interferometric technique for faceted microstructure metrology using an index matching liquid," Appl. Opt. **49**(4), 732–738 (2010).
5. F. Fang, Z. Zeng, X. Zhang, and L. Jiang, "Measurement of micro-V-groove dihedral using white light interferometry," Opt. Commun. **359**, 297–303 (2016).
6. F. Gao, J. Coupland, and J. Petzing, "V-groove measurements using white light interferometry," in *Photon06, Manchester*, (2006) pp. 4–7.
7. C. J. Evans and J. B. Bryan, "'Structured', 'textured' or 'engineered' surfaces," CIRP Ann. Manuf. Tech. **48**(2), 541–556 (1999).
8. L. Singleton, R. Leach, A. Lewis, and Z. Cui, "Report on the analysis of the MEMSTAND survey on Standardisation of MicroSystems Technology," MEMSTAND Project IST-2001- 37682 (2002).
9. B. F. Ju, Y. L. Chen, W. Zhang, and F. Z. Fang, "Rapid measurement of a high step microstructure with 90° steep sidewall," Rev. Sci. Instrum. **83**(1), 013706 (2012).
10. A. P. Tafti, A. B. Kirkpatrick, Z. Alavi, H. A. Owen, and Z. Yu, "Recent advances in 3D SEM surface reconstruction," Micron **78**, 54–66 (2015).
11. D. Malacara, *Optical shop testing* (John Wiley & Sons, 2007).
12. M. J. Jansen, H. Haitjema, and P. H. Schellekens, "Scanning wafer thickness and flatness interferometer," Proc. SPIE **5252**, 334–345 (2004).
13. X. Jiang, K. Wang, F. Gao, and H. Muhamedsalih, "Fast surface measurement using wavelength scanning interferometry with compensation of environmental noise," Appl. Opt. **49**(15), 2903–2909 (2010).
14. H. Muhamedsalih, F. Gao, and X. Jiang, "Comparison study of algorithms and accuracy in the wavelength scanning interferometry," Appl. Opt. **51**(36), 8854–8862 (2012).

15. M. Takeda and H. Yamamoto, "Fourier-transform speckle profilometry: three-dimensional shape measurements of diffuse objects with large height steps and/or spatially isolated surfaces," Appl. Opt. **33**(34), 7829–7837 (1994).
16. G. D. MacAulay, N. Senin, C. L. Giusca, and R. K. Leach, "Study of manufacturing and measurement reproducibility on a laser textured structured surface," Measurement **94**, 942–948 (2016).
17. G. D. MacAulay, N. Senin, C. L. Giusca, and R. K. Leach, "Comparison of segmentation techniques to determine the geometric parameters of structured surfaces," Surf. Topog. Metrol. Prop. **2**(4), 044004 (2014).

1. Introduction

Micro-fabricated structured surfaces with multi-side high sloped facets, such as micropyramidal arrays, V-grooves, prismatic films or lenslet arrays have found wide applications in optical industries such as optical communication, liquid crystal display (LCD), diffractive optics, micro optics, light guiding applications etc [1–7]. The manufactured items are reported to suffer from high scrap rates up to 50-70% since the fabrication is heavily reliant on the experience of the processing workers adopting an expensive trial-and-error approach [8]. Therefore overcoming this issue becomes increasingly meaningful.

Currently, it is challenging to measure the structured surfaces with multi-side high sloped facets to achieve high-precision topography, irrespective of whether using a contact or non-contact method. The stylus profilometer, for instance, can provide a nanometer resolution profile, but regarding areal measurement, the resolution decreases because of the jump between different profiles and it is also relatively time-consuming. As for microstructures with a high aspect ratio, the size of the stylus might induce large deviations. Furthermore, the stylus might damage the sample being inspected. Optical scanning techniques such as confocal microscopes and interferometers, are also restricted in this area, either the maximum measurement angle is limited by the numerical aperture (NA) [9], or the resolution is too low because the angle is too large when measuring structured surfaces with multi-side high sloped facets. Sometimes it is even impossible to measure the structured surfaces correctly, for example, Gao *et al.* reported some highly repeatable systematic errors with white light scanning interferometry (WLSI) [6]. SEM is capable of observing a variety of structures with high lateral resolution, however, it is not able to acquire the height information [10]. Even with the powerful Scanning Probe Microscope (SPM) family of instruments, including, Atomic Force Microscope (AFM) and Scanning Tunnel Microscope (STM), the axial range (normally just several microns) is still a bottleneck and restricts its application in this area [11]. Li *et al*. developed a compact and fast Autostereoscopy-based Three-Dimensional On-machine Measuring (ATDOM) system to achieve efficient in-situ measurement [2,3]. However, the low performance of measurement repeatability is a large limitation.. Jansen *et al.* presented a scanning double side Fizeau interferometer to simultaneously probe both the front and back sides of a silicon wafer to measure its thickness and flatness [12]. Although the system is for measuring two nearly parallel faces, it provides confidence that the acquisition of the topography of the structured surfaces with multi-side high sloped facets might be achieved by developing a measurement system composed of two or more interferometers.

Wavelength Scanning Interferometry (WSI) has many distinct features [13]. Firstly, compared to Vertical Scanning Interferometry (VSI), WSI requires no mechanical scanning, which means the probe is fixed during measurement and the scanning process could be very fast, with the potential of on-line measurement. Also the resolution is very high, which has been proved to reach nanometer axial resolution in previous research [13,14]. Consequently, WSI is adopted in this research to solve part of the challenge, i.e., to obtain the topography of the double-sided near-right-angle structured surfaces.

2. Methodology

System setup

The DPWSI system, as illustrated in Fig. 1, is mainly comprised of a tungsten-halogen bulb, an acousto optical tunable filter (AOTF) and two WSI probes or interference objectives which

are orthogonally placed for micro and nano-scale areal surface measurement. The AOTF filters the white light emanating from the tungsten-halogen bulb into a single-wavelength which is conducted through the fiber and then be split into two beams, illuminating the two interferometers respectively. By changing the frequency of the driving RF signal gradually, the wavelength scanning is achieved [13]. The two probes are identical and with a large working distance of 30 mm, enabling the measurement of large objects. Each of the probes forms an interferometer, which simultaneously measures the structured surface in two orthogonal directions. During the wavelength scanning process, 256 frames of interferograms are captured from each of the probes by the corresponding cameras, which are then analyzed by a fringe analysis algorithm such as the phase slope algorithm [14,15] to acquire the measurement volume information of each probe respectively. In order to build up the whole topography information of the measured sample the two measurement data sets should be bound together based on the space coordinate calibration using a specially designed calibration specimen and 3D registration algorithm. Since there is no overlapping measurement area between the two orthogonally placed interferometers, it is meaningless to point two interferometers at the same location. This means, the relative locations of the two interferometers have to be calibrated, otherwise, the measurement results of the two interferometers are totally independent and it is almost impossible to bind them together to form the whole topography.

Calibration principle

The interference microscope objectives in the measurement system adopt the Michelson interferometer setup. As illustrated in Fig. 2, the light beams reflected from the reference mirrors REF1 and REF2 interfere with the light beams reflected from the sample correspondingly. The measurement result acquired from each interferometer is half of the optical path difference (OPD) between the sample surface to the corresponding virtual image of the reference plane, in other words, the measurement results have a fixed relationship with respect to the locations of the two virtual images of the reference mirrors, namely VREF1 and VREF2. Since there is no mechanical movement during the measurement process, the reference mirrors REF1, REF2 and the beam-splitters BS1, BS2 remain static to each other throughout the process. Therefore the relationship between the two probes can be established through the space coordinate calibration, then the whole topography of the sample can be obtained.
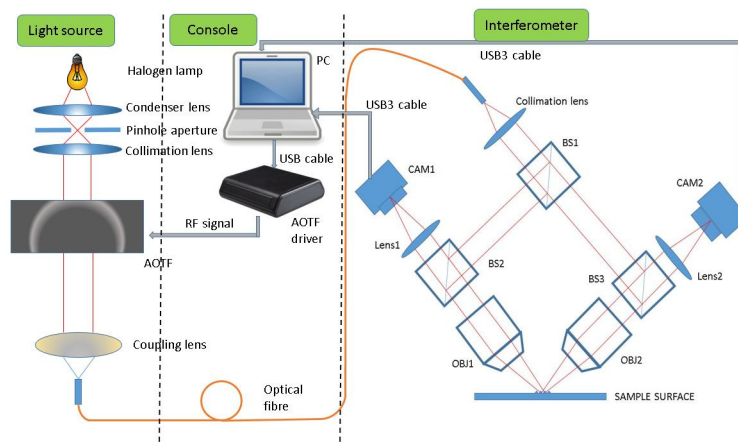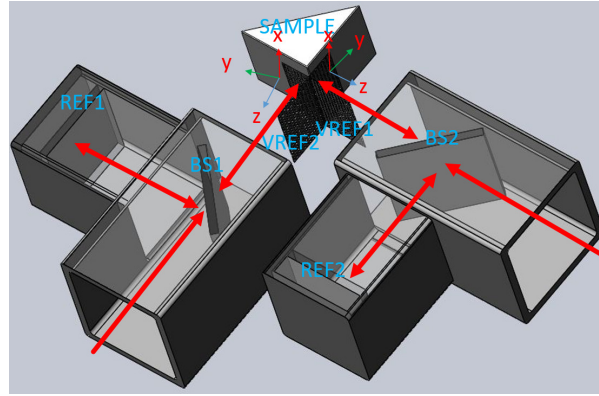

Fig. 1. Block diagram of the setup.

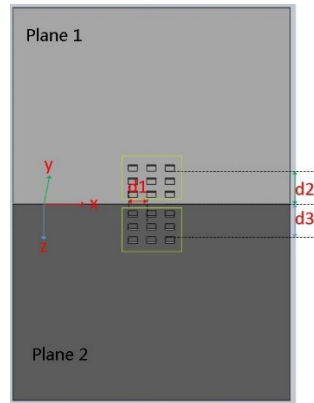Fig. 2. The coordinate system of the probes.

Fig. 3. The relative location of the 2 faces of the artefact.

If P_n, $P_n^{'}$ represent the quaternions of the feature points such as corners or centers of the features in the reference topography, and Q_n, $Q_n^{'}$ represent the quaternions of the corresponding feature points in the measurement results by the 2 probes respectively. The following equations must be satisfied:

$$\begin{pmatrix} R_1 & t_1 \\ 0 & 1 \end{pmatrix} Q_n^{'} = P_n^{'}. \tag{1}$$

$$\begin{pmatrix} R_2 & t_2 \\ 0 & 1 \end{pmatrix} Q_n = P_n. \tag{2}$$

$$R_n = \begin{pmatrix} 1 & 0 & 0 & 0 \\ 0 & \cos\alpha_n & \sin\alpha_n & 0 \\ 0 & -\sin\alpha_n & \cos\alpha_n & 0 \\ 0 & 0 & 0 & 1 \end{pmatrix} * \begin{pmatrix} \cos\beta_n & 0 & -\sin\beta_n & 0 \\ 0 & 1 & 0 & 0 \\ \sin\beta_n & 0 & \cos\beta_n & 0 \\ 0 & 0 & 0 & 1 \end{pmatrix} * \begin{pmatrix} \cos\gamma_n & \sin\gamma_n & 0 & 0 \\ -\sin\gamma_n & \cos\gamma_n & 0 & 0 \\ 0 & 0 & 1 & 0 \\ 0 & 0 & 0 & 1 \end{pmatrix}. \tag{3}$$

$$t_n = \begin{pmatrix} t_{nx} & t_{ny} & t_{nz} \end{pmatrix}. \tag{4}$$

where R_1, R_2 refer to the rotation matrices from the coordinate systems of the two probes to the reference topography, while t_1, t_2 represent the translation matrices from the coordinate systems of the two probes to the reference topography, α_n, β_n, γ_n represent the rotation angles between the coordinate systems around the x, y, z axes, t_{nx}, t_{ny}, t_{nz} refer to the translation components along the x, y, z axes. So there are 12 unknown variables in total. Theoretically if there are enough pairs of irrelevant feature points, i.e. more than four pairs (since three equations can be obtained with each pair of feature points), the matrices will be able to be determined. The feature points can be extracted with an image processing algorithm from the measurement results by WLSI (Taylor Hobson CCI 3000), SEM and DPWSI respectively with the edge extraction method described in [16,17] such as Sobel operator and Watershed. The spike errors, like batwing, might be a problem so a cluster filter is used to remove the outliers before the extraction. These equations can be theoretically solved with Procrustes operation in MATLAB. However, since errors inevitably exist when extracting the feature points, a 3D registration algorithm such as Iterative Closest Points (ICP) is used to improve the matching accuracy. Since the data sets are treated as a whole in ICP algorithm, it is difficult to match the features accurately unless all the features are first extracted before using the algorithm for matching, which means, the fabrication quality of the features has large impact on the calibration accuracy. After solving these equations, the coordinate systems of the two interference probes are established. After that, the two data sets acquired from the two probes can be bound together to form the whole topography of the structured surface as:

$$\begin{pmatrix} \begin{pmatrix} R_1 & t_1 \\ 0 & 1 \end{pmatrix} X \\ \begin{pmatrix} R_2 & t_2 \\ 0 & 1 \end{pmatrix} Y \end{pmatrix} \rightarrow \begin{pmatrix} \begin{pmatrix} R_1 & t_1 \\ 0 & 1 \end{pmatrix}^{-1} \begin{pmatrix} R_1 & t_1 \\ 0 & 1 \end{pmatrix} X \\ \begin{pmatrix} R_1 & t_1 \\ 0 & 1 \end{pmatrix}^{-1} \begin{pmatrix} R_2 & t_2 \\ 0 & 1 \end{pmatrix} Y \end{pmatrix} = \begin{pmatrix} X \\ \begin{pmatrix} R_1 & t_1 \\ 0 & 1 \end{pmatrix}^{-1} \begin{pmatrix} R_2 & t_2 \\ 0 & 1 \end{pmatrix} Y \end{pmatrix}. \qquad (5)$$

where X refers to the result measured with probe 1, while Y represents the result acquired with probe 2. To reduce the computation, the result can be rotated and translated in the same coordinate system as shown above without changing the result.

The artefact is a certified calibration-standard cube, with two adjoining faces perpendicular to each other within two seconds of arc (the real deviation is 1.2 arcsecs measured with autocollimator). The roughness and flatness of the two faces are both very high (S_a better than 30 nm, flatness better than 50 nm) and the edge between the two faces is very sharp. The features were milled with Focused Ion Beam (FIB) with a depth between 200 and 300 nm. To our knowledge from both the literature and experiment, none of the existing instruments are able to acquire the topography of the structured surface of the artefact with sufficient resolution to detect the features. The reference topography is reconstructed by combining the results acquired with Taylor Hobson CCI 3000 and FEI Quanta 200 3D FIB/SEM workstation with the method illustrated in Fig. 3. The areas including the features on both facets (illustrated as the two rectangles in Fig. 3) can be measured with a Taylor Hobson CCI 3000 with nanometer scale vertical resolution. The relative location between the two faces can be measured with SEM with submicron resolution, acquiring the distances d_1, d_2 and d_3 in three different directions as shown in Fig. 3. With the angle between the two planes, the topography can be reconstructed by stitching the data together based on the coordinate system shown in Fig. 3 with the following restrictions:

$$\begin{cases} distance\left(f_{1,p_1}, f_{1,p_2}\right) = d_1 \\ distance\left(f_{2,p_1}, p_2\right) = d_2 \\ distance\left(f_{2,p_2}, p_1\right) = d_3 \end{cases}. \tag{6}$$

where P_n refers to the fitted plane of face n = 1 or 2, f_{m,p_n} represents the selected feature on plane P_n, m = 1 or 2. The stitching can be accomplished by keeping the data of one face still, rotate and translate the other face to satisfy these restrictions with only rigid transformations.

3. Experimental results and discussions

Both the two probes of the DPWSI have been calibrated with the step-height standard specimens. The result shows each probe has achieved nanometer scale vertical accuracy. As an example, Fig. 4 is the measurement result of a 178 nm step-height sample manufactured by VLSI standards measured by one of the probes, the deviation is only several nanometers. The result of the other probe is very similar.
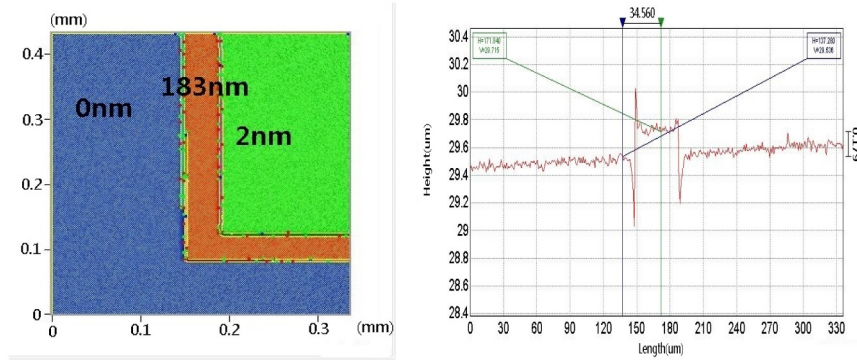

Fig. 4. The measurement result of a 178 nm standard step-height sample by one of the probes.

The reference topography of the coordinate relationship calibration artefact has been stitched and the system has been calibrated. The stitched result by the DPWSI is shown in Fig. 5(a) with the residual error illustrated in Fig. 5(b). The residual error of the majority of points (99.96%) is below 4 μm which is about the lateral resolution of the interferometers, only a small number of the points (0.04%) at the edge of the features with spike errors such as batwing the residual error exceeds 4 μm. A series of the profiles are shown in Fig. 5(c) separated with a certain gap in blue. Since the depth of the features (200-300 nm) is tiny compared to the other dimensions, the depth of the features are enlarged to ensure the features can be seen. A profile with true measurement data is also provided for the top and side face respectively in red. The experiment shows it is very difficult to align the data sets directly with ICP algorithm. The best way to make the alignment is to extract the features in the data sets first, and then make alignment with the corresponding features. The 3D registration result between Taylor Hobson CCI 3000 and both DPWSI probes shows the average deviation between the matched areas is micrometer scale in the lateral direction and submicron level in the axial direction. There are many reasons for the deviation. The spike errors, like batwing, are an important error source, but can be eliminated by the cluster filter and outlier removal algorithm. The imperfect surface finish of the bottom of the features is another error source, which causes difference between the instruments because the numerical aperture (NA) of the objectives of Taylor Hobson CCI 3000 and DPWSI are different. However, the error can be reduced if the fabrication quality of the calibration artefact could be improved and more features are manufactured and adopted. Despite all of these error sources, the average lateral

deviation of the registration is micrometer level, which is similar to the lateral resolution of the probes (about 4 μm). Since only rigid transformations are adopted in the registration, the shape of the two faces are not changed, thus the vertical resolution of the two faces remains the same in nanometer scale after the stitching but with the relative locations of the two faces distorted by micrometer level. The dihedral between the two faces is calculated with a result of 89.9646°. The deviation compared to the result measured by autocollimator is 2.144 arcmins which is quite large and is partially attributable to the fabrication quality of the calibration artefact and can be improved by reforming the calibration artefact.
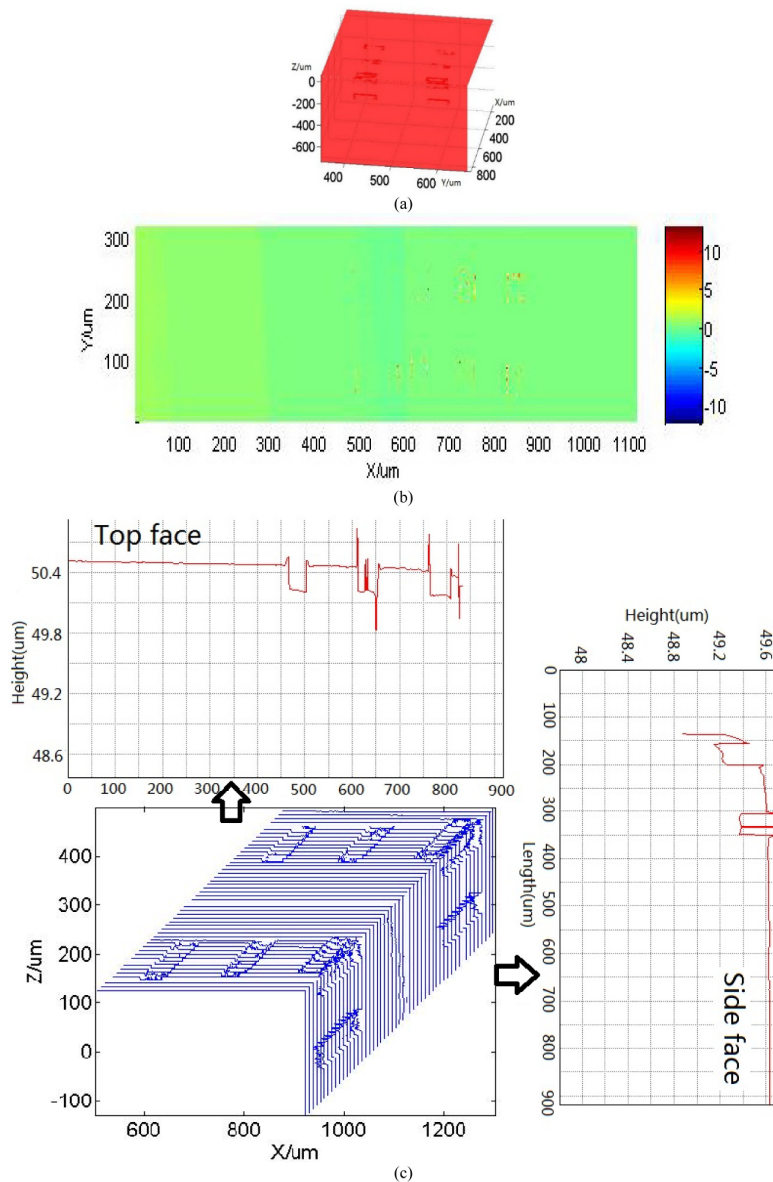
Fig. 5. (a) The topography measured with the DPWSI. (b) The residual error of the topography compared to the reference topography measured with Taylor Hobson CCI 3000 and FEI Quanta 200 3D FIB/SEM workstation. (c) The extended 2D plots of the DPWSI topography.

Two samples were measured to test the capability of the proposed method. One sample is a cylindrical diamond-turned multi-step specimen with 20 µm step height and the diameter about 20 mm, as shown in Fig. 6. Due to the edge and slope effects some of the measurement data are lost in the edge and high-sloped area. As a comparison, Fig. 7 is the measurement result of the same specimen by Taylor Hobson CCI 3000, which agrees with the DPWSI result exactly. The only problem is it only provides the information in one direction and with totally no information about the side face.

(a) Probe 1   (b) Probe 2

(c) Stitched result
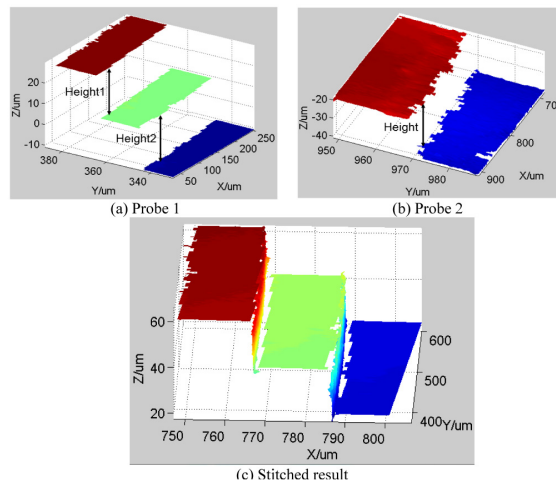
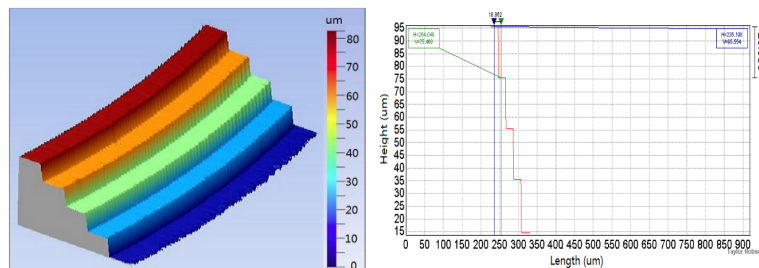Fig. 6. The measurement result of the diamond turned specimen by DPWSI.

Fig. 7. The measurement result of the diamond turned specimen by Taylor Hobson CCI 3000.

Another sample is a metallized prismatic film manufactured by Microsharp, the result is shown in Fig. 8. As can be seen, the height of the steps is around 32 µm. It can also be seen that the high curvature areas, i.e., the peaks and valleys are still not measured because the surface normals in those areas scatter light beyond the NA of the corresponding interference objectives. Figure 9 is a comparison of the measurement results of the same film by the DPWSI and a stylus profilometer (Taylor Hobson PGI Form Talysurf Series 2 with the radius of the stylus tip only 2 µm). As can be seen, the DPWSI profile has sharp peaks and valleys, which is because the measurement data on the edges of the surface is missing and interpolated data is used. Whereas the measurement result of the stylus profilometer is circular at the top edge which is confirmed to be sharp by SEM because of the affection caused by the tip size of the stylus. The result of the stylus profilometer which is corrected by deconvolution of the stylus tip radius is shown by the blue profile in Fig. 9(b) but the improvement is limited. Overall, except for the areas at the edge, the DPWSI result agrees with the result measured by a stylus profilometer very well.
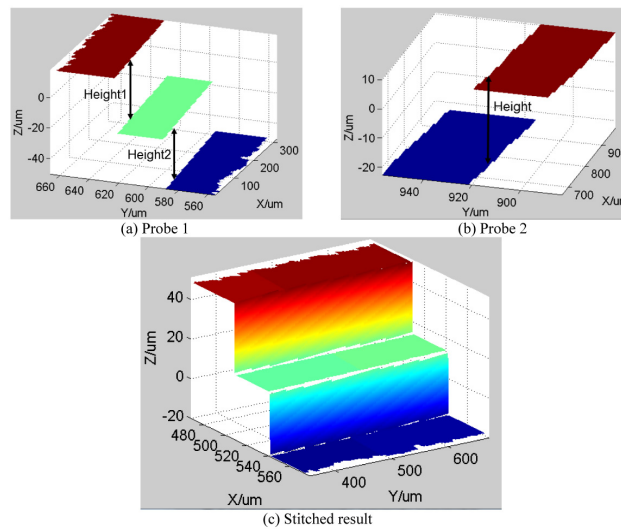
(a) Probe 1

(b) Probe 2

(c) Stitched result

Fig. 8. The measurement result of a metallised prismatic film.
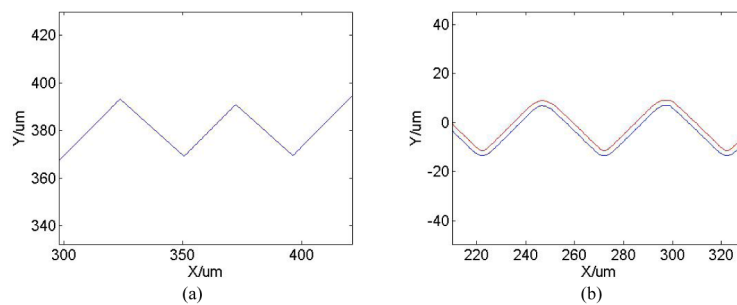

(a)

(b)

Fig. 9. The comparison of the measurement results of the metallised prismatic film by: (a) DPWSI and (b) Taylor Hobson PGI Form Talysurf Series 2, red is before deconvolution, blue is after deconvolution.

To conclude, the experimental result shows the proposed measurement system has demonstrated a novel approach to measure structured surfaces with double-sided near-right-angle facets and output the topography with nanometer scale vertical resolution on each facet and micrometer scale lateral resolution. Most of the surface information can be provided except for the parts of the surfaces with the normals scattering light beyond the NA of the probes and all the surface parameters such as S_a, S_q, S_z and flatness etc. can be calculated from the topography.

Funding

Acknowledgment